Path Integral Monte Carlo on a Sphere

Riccardo Fantoni*
Università di Trieste, Dipartimento di Fisica, strada Costiera 11, 34151 Grignano (Trieste), Italy
(Dated: February 16, 2026)

...

Keywords: Path Integral; Monte Carlo; Sphere

CONTENTS

I. INTRODUCTION

Sphere [1, 2], Haldane sphere [3–5] ...

II. MANY BODY PATH INTEGRAL ON A RIEMANNIAN MANIFOLD

A many body system is composed of N *distinguishable* particles of mass m and spin s with positions in $R = (\boldsymbol{r}_1, \boldsymbol{r}_2, \ldots, \boldsymbol{r}_N) = (\{\boldsymbol{r}_i\})$ where each position vector $\boldsymbol{r}_i = (r_i^1, r_i^2, \ldots, r_i^d) = (\{r_i^\alpha\})$ in d dimensions. On a Riemannian manifold $\mathscr{M}$ of dimension d and metric tensor $g_{\alpha\beta}(\boldsymbol{r})$, the geodesic distance between two infinitesimally close points

* riccardo.fantoni@scuola.istruzione.it

R and R' is $d\tilde{s}^2(R,R') = \sum_{i=1}^N ds^2(\boldsymbol{r}_i,\boldsymbol{r}'_i)$ where $ds^2(\boldsymbol{r},\boldsymbol{r}') = g_{\alpha\beta}(\boldsymbol{r})(\boldsymbol{r}-\boldsymbol{r}')^\alpha(\boldsymbol{r}-\boldsymbol{r}')^\beta$. Moreover,

$$\tilde{g}_{\mu\nu}(R) = g_{\alpha_1\beta_1}(\boldsymbol{r}_1)\otimes\ldots\otimes g_{\alpha_N\beta_N}(\boldsymbol{r}_N), \tag{2.1}$$

$$\tilde{g}(R) = \prod_{i=1}^N \det||g_{\alpha_i\beta_i}(\boldsymbol{r}_i)||, \tag{2.2}$$

where $||\tilde{g}_{\mu\nu}||$ is a matrix made of N diagonal blocks $||g_{\alpha_i\beta_i}||$ with $i=1,2,\ldots,N$. The Laplace-Beltrami operator on the manifold of dimension dN is

$$\Delta_R = \tilde{g}^{-1/2}\nabla_\mu(\tilde{g}^{1/2}\tilde{g}^{\mu\nu}\nabla_\nu), \tag{2.3}$$

where $\nabla = \nabla_R$, $\tilde{g}^{\gamma\nu}$ is the inverse of $\tilde{g}_{\gamma\nu}$, i.e. $\tilde{g}_{\mu\gamma}\tilde{g}^{\gamma\nu} = \delta_\mu{}^\nu$ the Kronecker delta, and a sum over repeated indexes is tacitly assumed.

We will first assume *free*, non interacting bodies, with an Hamiltonian $\mathscr{H}$ that reduces to the one of the free gas in flat space. For the sake of simplicity [1] we will choose

$$\mathscr{H} = -\lambda\Delta_R, \tag{2.4}$$

with $\lambda = \hbar^2/2m$.

For *interacting* bodies we will then have more generally

$$\mathscr{H} = -\lambda\Delta_R + V(R), \tag{2.5}$$

where V is the potential energy of the system, that we here assume only a function of the particles positions and bounded from below.

The density matrix ρ of the system obeys Bloch equation

$$\frac{\partial\rho(t)}{\partial t} = -\mathscr{H}\rho(t), \tag{2.6}$$

$$\rho(0) = \mathbb{1}, \tag{2.7}$$

where t is the imaginary time with the dimensions of an energy and $\mathbb{1}$ the identity matrix. The position representation of the density matrix is then obtained from $\rho(R,R';t) = \langle R|\rho(t)|R'\rangle$ with $\langle R|R'\rangle = \delta(R-R')/\sqrt{\tilde{g}(R)}$ where δ is a dN dimensional Dirac delta function. In the small imaginary time τ limit the position representation of the density matrix is

$$\rho(R,R';\tau) \propto \tilde{g}(R)^{-1/4}\sqrt{\mathscr{D}(R,R';\tau)}\,\tilde{g}(R')^{-1/4}e^{\lambda\tau\mathscr{R}(R)/6}e^{-\mathscr{S}(R,R';\tau)}, \tag{2.8}$$

where $\mathscr{R}$ is the scalar curvature of the manifold [2], $\mathscr{S}$ the action, and $\mathscr{D}$ the van Vleck's determinant [8, 9]

$$\mathscr{D}_{\mu\nu} = -\nabla_\mu\nabla'_\nu\mathscr{S}(R,R';\tau), \tag{2.9}$$

$$\det||\mathscr{D}_{\mu\nu}|| = \mathscr{D}(R,R';\tau), \tag{2.10}$$

where $\nabla = \nabla_R$ and $\nabla' = \nabla_{R'}$. This determinant is the Jacobian of the transformation from the initial conditions given by fixing the pair of momentum and coordinate to the boundary conditions given by specifying the pair of initial and final coordinates needed in the path integral formulation. For the density matrix (2.8) the volume element for integration is $\sqrt{\tilde{g}(R)}\,dR$. The two factors $\tilde{g}^{-1/4}$ are needed in order to have for the density matrix a bidensity for which the boundary condition to Bloch equation is simply a Dirac delta function $\rho(R,R';0) = \delta(R-R')$. The square root of the van Vleck determinant factor takes into account the density of paths among the minimum extremal region for the action (see Chapter 12 of Ref. [9]).

For the *action* $\mathscr{S}$, the *kinetic-action* $\mathscr{K}$, and the *inter-action* $\mathscr{U}$ we have [3]

$$\mathscr{S}(R,R';\tau) = \mathscr{K}(R,R';\tau) + \mathscr{U}(R,R';\tau), \tag{2.11}$$

$$\mathscr{K}(R,R';\tau) = \frac{dN}{2}\ln(4\pi\lambda\tau) + \frac{d\tilde{s}^2(R,R')}{4\lambda\tau}. \tag{2.12}$$

---

[1] This is a delicate point and should be studied more carefully [6]. Especially for what concerns ordering ambiguities. We here appeal to simplicity.

[2] The factor depending on the curvature of the manifold is due to Bryce DeWitt [7]. For a space of constant curvature there is clearly no effect, as the term due to the curvature just leads to a constant multiplicative factor that has no influence on the measure of the various observables.

[3] The expression for $\mathscr{K}$ is the one of Eq. (24.16) of Ref. [9] to lowest order in $R-R'$.

In particular the kinetic-action is responsible for a diffusion of the random walk with a single particle variance on the α, β components equal to $\sigma^2_{\alpha\beta}(\boldsymbol{r}) = 2\lambda\tau/g_{\alpha\beta}(\boldsymbol{r})$. The inter-action is defined as $\mathscr{U} = \mathscr{S} - \mathscr{K}$ and for potential energies bounded from below one can resort to Trotter formula [10] to reach the *primitive approximation* [4]

$$\mathscr{U}(R, R'; \tau) = \tau[V(R) + V(R')]/2. \tag{2.13}$$

For non interacting bodies $\mathscr{U} = 0$. Note that, even to lowest order in $R - R'$ [5], the path integral in the curved manifold for the non interacting system will not coincide with the one in flat space since it is not possible with a change of coordinates to simply remove the metric factor from both $d\tilde{s}^2$ and the volume element of integration, if not only locally. In fact this would require a *non coordinate basis* [13].

Given then an observable $\mathscr{O}$ we can determine its thermal average at an absolute temperature T from

$$\langle \mathscr{O} \rangle = g_s \mathrm{tr}\{\rho(\beta)\mathscr{O}\}/Z_N, \tag{2.14}$$

$$Z_N = g_s \mathrm{tr}\{\rho(\beta)\}, \tag{2.15}$$

where $\beta = 1/k_B T$ with k_B Boltzmann constant, $\mathrm{tr}\{\ldots\}$ is the trace over the spatial variables, Z_N the canonical partition function, $g_s = 2s + 1$ is the spin degeneracy, and we assumed the Hamiltonian independent from spin. *Spinless* bodies have $g_s = 1$. Actually the spin-statistics theorem of quantum field theory, dictates that in spatial dimension bigger than two, particles with integer spin are bosons (obeying Bose-Einstein statistics, symmetric wavefunctions), while half-integer spin particles are fermions (obeying Fermi-Dirac statistics, antisymmetric wavefunctions). In dimension two anyonic statistics are also possible.

The position representation of the density matrix at an imaginary time $t = \beta$ is obtained through a path integral

$$\rho(R, R'; \beta) = \langle R|\rho(\beta)|R'\rangle = \int \prod_{k=0}^{M-1} [\rho(R_k, R_{k+1}; \tau)\, dR_k]\, \delta(R_0 - R)\delta(R_M - R')\, dR_M, \tag{2.16}$$

where we have discretized the imaginary time β into M *timeslices* with a small *timestep* $\tau = \beta/M$, a *bead* $R_k = (\{\boldsymbol{r}_{i,k}\}) = (\{r^\alpha_{i,k}\})$ at each timeslice $k = 1, 2, \ldots, M$. We will also call *link* a pair of contiguous beads. Note that in order to measure an observable through Eq. (2.14) it is necessary to consider closed paths such that $R(t + \beta) = R(t)$, or rings on the manifold $\mathscr{M}$.

For *identical* bodies if they satisfy to the Bose-Einstein statistics one needs to symmetrize the distinguishable density matrix, if they satisfy to the Fermi-Dirac statistics one needs to antisymmetrize it [14]. In these cases we can then write [6]

$$\rho_\pm(R, R'; \beta) = \frac{1}{N!} \sum_{\mathscr{P}} \mathrm{sgn}(\mathscr{P}) \rho(\mathscr{P}R, R'; \beta), \tag{2.17}$$

$$\mathrm{sgn}(\mathscr{P}) = (\pm 1)^{\sum_{\nu=1}^{N} (\nu-1) C_\nu}, \tag{2.18}$$

where $\mathscr{P}$ is any permutation of the N particles such that $\mathscr{P}R = (\boldsymbol{r}_{\mathscr{P}1}, \boldsymbol{r}_{\mathscr{P}2}, \ldots, \boldsymbol{r}_{\mathscr{P}N})$, with sign $\mathrm{sgn}(\mathscr{P})$. Any permutations can be broken into cycles $\mathscr{P} = \{C_\nu\}$ where C_ν is the number of cycles of length ν in $\mathscr{P}$. In the sum over the permutation one should use a $+1$ for the symmetrization necessary for bosons and -1 for the antisymmetrization necessary for fermions, in $\mathrm{sgn}(\mathscr{P})$.

On a surface, $d = 2$, for *impenetrable* identical bodies, one can also have anyonic statistics [15]. In this case it is necessary to consider, more generally,

$$\rho_\nu(R, R'; \beta) = \sum_{\alpha \in B_N} \mathrm{Re}[\chi(\alpha)] \rho_\alpha(R, R'; \beta), \tag{2.19}$$

$$\chi(\text{paths } R(t) \text{ with } n \text{ braids among the pairs of single particle paths } \boldsymbol{r}(t)) = e^{-i\nu n\pi}, \tag{2.20}$$

where B_N is the infinite braid group which admits an infinite number of unitary one dimensional representations χ parametrized by an arbitrary number ν which determines the statistics and ρ_α is the distinguishable density matrix obtained from paths of kind α only. Clearly for $\nu = 0$ we recover the Bose-Einstein statistics and for $\nu = 1$ the Fermi-Dirac statistics. So we will be interested in values of $0 < \nu < 1$.

The braid group is the fundamental group of the quotient space $(S^{2N} - \Delta)/S_N$ where S^2 is the (two) sphere, $\Delta = \{R \mid \boldsymbol{r}_i = \boldsymbol{r}_j \text{ for some } i \neq j\}$, and S_N is the group of permutation of N bodies. We then see how paths $R(t)$ with different numbers of crossings between single particle paths $\boldsymbol{r}(t)$ belong to different homotopy classes and one cannot be deformed continuously into the other. Therefore in order to take care of the density matrix of identical impenetrable bodies it is necessary to sum over all the topologically disjoint homotopy classes as is done in Eq. (2.19).

---

[4] See Ref. [11] for a numerical analysis of the accuracy of this approximation and for possible its refinements.

[5] For next orders corrections see for example Ref. [12].

[6] One can symmetrize or antisymmetrize respect to the first, the second or both the arguments of the distinguishable density matrix. We here choose the first case.

III. THE SPHERE

A sphere of radius a is the surface, $d = 2$ [7], with metric $ds^2 = g_{\alpha\beta}dr^\alpha dr^\beta = a^2(d\theta^2 + \cos^2\theta\, d\varphi^2)$, [8] of constant positive scalar curvature $2/a^2$ so that $\mathscr{R} = 2N/a^2$. The polar angle $r^1 = \theta \in]-\pi/2, \pi/2]$ and the azimuthal angle $r^2 = \varphi \in]-\pi, \pi]$ are the contravariant coordinates of the position vector $\boldsymbol{r} \in \mathscr{C}$ with $\mathscr{C} =]-\pi/2, \pi/2] \times]-\pi, \pi]$ the single particle consfiguration space. On the sphere $\sqrt{g(\boldsymbol{r})} = a^2|\cos\theta|$ and in the small $\tau \to 0$ limit [9] $\tilde{g}(R)^{-1/4}\sqrt{D(R, R'; \tau)}\,\tilde{g}(R')^{-1/4} \to (1/2\lambda\tau)^N$. So we see how both the curvature term and the van Vleck factor, being constant, simply drop off from the measure of the various observables of Eq. (2.14).

The position of a particle on the sphere in the three dimensional Euclidean space embedding the sphere is

$$\begin{cases} x = a\cos\theta\cos\varphi \\ y = a\cos\theta\sin\varphi \\ z = a\sin\theta \end{cases} \tag{3.1}$$

and the particle path in it is $\boldsymbol{q}(t) = (x(t), y(t), z(t))$.

The geodesic distance between particles $\boldsymbol{r}_i$ and $\boldsymbol{r}_j$ is

$$s_{ij} = s(\boldsymbol{r}_i, \boldsymbol{r}_j) = a\arccos\left[\sin(r_i^1)\sin(r_j^1) + \cos(r_i^1)\cos(r_j^1)\cos(r_i^2 - r_j^2)\right], \tag{3.2}$$

whereas the Euclidean distance is

$$d_{ij} = d(\boldsymbol{r}_i, \boldsymbol{r}_j) = a\sqrt{2(1 - \hat{\boldsymbol{q}}_i \cdot \hat{\boldsymbol{q}}_j))} = 2a\sin[\arccos(\hat{\boldsymbol{q}}_i \cdot \hat{\boldsymbol{q}}_j)/2]., \tag{3.3}$$

where $\hat{\boldsymbol{q}}_i = \boldsymbol{q}_i/a$ is the versor that from the center of the sphere points towards the center of the ith particle.

We use the Metropolis algorithm [16, 17] to evaluate the average of Eq. (2.14). In order to explore ergodically the configuration space $\boldsymbol{r} = (\theta, \varphi) \in \mathscr{R}$ to sample the distinguishable density matrix we use the transition *displacement* move described in Appendix A. In order to sample the permutation sum of Eq. (2.17) needed for identical bodies we use a transition move combination of 2 Brownian *bridges* between unlike bodies as described in Appendix B. Note that even if the kinetic action $d\tilde{s}^2(R, R')$ is not really quadratic due to the presence of the metric factors, nonetheless in the high temperature limit $\tau \to 0$, neededed in the path integral (2.16) it is still possible to consider it as quadratic in R at fixed R' or viceversa. In order to sample the sum over the homotopy classes of Eq. (2.19) needed for identical impenetrable bodies we use a combination of bridge and displacement transition moves as described in Appendix C. Note that the displacement moves can be freely substituted by moves of bridges connecting only like bodies. But we found them still useful from a purely formal point of view where one starts from simple single bead moves and only later builds more complex many beads moves. Moreover since the single bead displacement move is simple to construct it can serve as a test upon the employment of many beads moves.

We will work in the canonical ensemble with fixed number of particles N, surface area $A = 4\pi a^2$, surface density $\sigma = N/4\pi a^2$, and absolute temperature $T = 1/k_B\beta$. The many body system *degeneracy parameter* is $\Theta = T/T_D$ where the degeneracy temperature $T_D = \sigma\hbar^2/mk_B$. For temperatures higher than T_D, $\Theta \gg 1$, quantum effects are less relevant. We will treat both the non interacting fluid $V = 0$ and the Coulomb fluid

$$V(R) = \sum_{i<j} \frac{e^2}{d_{ij}}, \tag{3.4}$$

where e is the unit of charge and we are assuming that the particles, moving on the sphere, interact with the three dimensional Coulomb potential [10]. The *Coulomb coupling constant* is $\Gamma = \beta e^2/a_0 r_s$ with $a_0 = \hbar^2/me^2$ the Bohr radius and the Wigner-Seitz radius $r_s = (4\pi\sigma)^{-1/2}/a_0$. At weak coupling, $\Gamma \ll 1$, the plasma becomes weakly correlated and approach the ideal gas limit. This will occur at high temperature and/or low density.

Choosing length in units of Wigner-Seitz radius, $a_0 r_s = a/\sqrt{N}$, and energy in units of Rydberg, $\mathrm{Ry} = \hbar^2/2ma_0^2$, we have $\lambda = \mathrm{Ry}/r_s^2$, $\Gamma = \beta(2/r_s)$, and $\Theta = (2\pi r_s^2)/\beta$. In this work we will choose units so that $\hbar = k_B = 1$.

Apart from the *kinetic energy* per particle e_K and the *potential energy* per particle e_V [11] we will also measure the *radial distribution function*, $g(r) = \langle\mathscr{O}\rangle$ for which we may use the following histogram estimator,

$$O(R; r) = \sum_{i\neq j} \frac{1_{]r-\Delta/2, r+\Delta/2]}(d_{ij})}{N n_{id}(r)}, \tag{3.5}$$

---

[7] So it is conformally flat as any Riemannian manifold of dimension $d \leq 3$.

[8] Note that in the kinetic action of the path integral Monte Carlo calculation it is crucial to use consistently either $ds^2(\boldsymbol{r}, \boldsymbol{r}') = g_{\alpha\beta}(\boldsymbol{r})(\boldsymbol{r} - \boldsymbol{r}')^\alpha(\boldsymbol{r} - \boldsymbol{r}')^\beta$ or $ds^2(\boldsymbol{r}, \boldsymbol{r}') = g_{\alpha\beta}(\boldsymbol{r}')(\boldsymbol{r} - \boldsymbol{r}')^\alpha(\boldsymbol{r} - \boldsymbol{r}')^\beta$.

[9] Remember that the metric tensor is covariantly cosntant.

[10] Note that this is not the only possible choice since we could as well choose particles "living in" [18] the surface of the sphere as done for example in Ref. [19–21].

[11] The estimators for these observables are carefully described in Ref. [11].

where Δ is the histogram bin, $1_{]a,b]}(x) = 1$ if $x \in]a, b]$ and 0 otherwise, and

$$n_{id}(r) = N \left[\left(\frac{r + \Delta/2}{2a} \right)^2 - \left(\frac{r - \Delta/2}{2a} \right)^2 \right] , \tag{3.6}$$

is the average number of particles on the spherical crown $]r - \Delta/2, r + \Delta/2]$ for the ideal gas of density σ. We have that $\sigma^2 g(r)$ gives the probability, that sitting on a particle at $\boldsymbol{r}$, one finds another particle at $\boldsymbol{r'}$ with $r = d(\boldsymbol{r}, \boldsymbol{r'}) \in [0, \sqrt{2a^2}]$, where $\sqrt{2a^2}$ is the Euclidean distance between a pole and a point on the equator. Alternatively one could consider a radial distribution function defined through the geodesic distance $r = s(\boldsymbol{r}, \boldsymbol{r'}) \in [0, \pi a/2]$ where one chooses $1_{]r-\Delta/2, r+\Delta/2]}(s_{ij})$ in Eq. (3.5) with an appropriate normalization [12].

For e_K and e_V we will use the *direct* estimator described in Ref. [11] applied to our action of Eq. (2.11).

In Table I we list some case studies treated by our computer experiments.

TABLE I. Cases treated in our simulations: a the sphere radius, N the number of particles, β the inverse temperature, $e_K = \langle \mathscr{K} \rangle$ the kinetic energy per particle from the thermodynamic estimator as explained in Ref. [11], and $e_V = \langle \mathscr{U} \rangle$ the potential energy per particle. The other quantities were introduced in the main text. In the statistics column "D" stands for distinguishable, "B" for bosons, "F" for fermions, and a numbre $\nu \in]0, 1[$ for anyons. We chose units with $\hbar = k_B = 1$.

case	statistics	M	N	a	$a/\sqrt{N}$	β	Γ	Θ	e_K	e_V
A	D	50	10	5	1.581	10	0	π	1.04(4)	0
B	B $\nu = 0$	50	10	5	1.581	10	0	π	-0.066(6)	0
C	F $\nu = 1$									
D	$\nu = 1/2$									
E	F $\nu = 1$	50	10	5	1.581	10	$6.324 \times e^2$	π		
...										

IV. NON INTERACTING BODIES

Here we will study non interacting spinless, $s = 0$, bodies with $\Gamma = 0$ or more generally $V = 0$.

A. Distinguishable bodies

Here we use the Metropolis algorithm with the transition displacement moves of Eqs. (A1) and (A2) or equivalently bridge moves of Eqs. (B1) and (B2) but between like particles.

In Fig. 1 we show a snapshot during the simulation for distinguishable non interacting particles with $M = 50, N = 10, a = 5, \beta = 1/10$.

In Fig. 2 we show the radial distribution function, calculated by averaging the estimator of Eq. (3.5), for the distinguishable non interacting gas with $N = 10$ on a sphere of radius $a = 5$ at an inverse temperature $\beta = 1/10$ with $M = 50$. This is the same configuration used for Fig. 1. As expected the radial distribution function is $g(r) = 1 - 1/N$ for $r < \sqrt{2a^2}$, where the $1/N$ term takes care of the finite size of the system. For $r > \sqrt{2a^2}$, i.e. for particles at a distance greater than the distance between the pole and a point on the equator, $g(r)$ increases, cheasing to be constant, due to the choice of using the Euclidean distance as in Eq. (3.5).

B. Identical bodies

Here we use the Metropolis algorithm with the transition displacement moves of Eqs. (A1) and (A2) and bridge moves of Eqs. (B1) and (B2) between unlike particles as described in Appendix B to produce the necessary particles exchanges.

[12] In Ref. [1] we used the Euclidean distance.

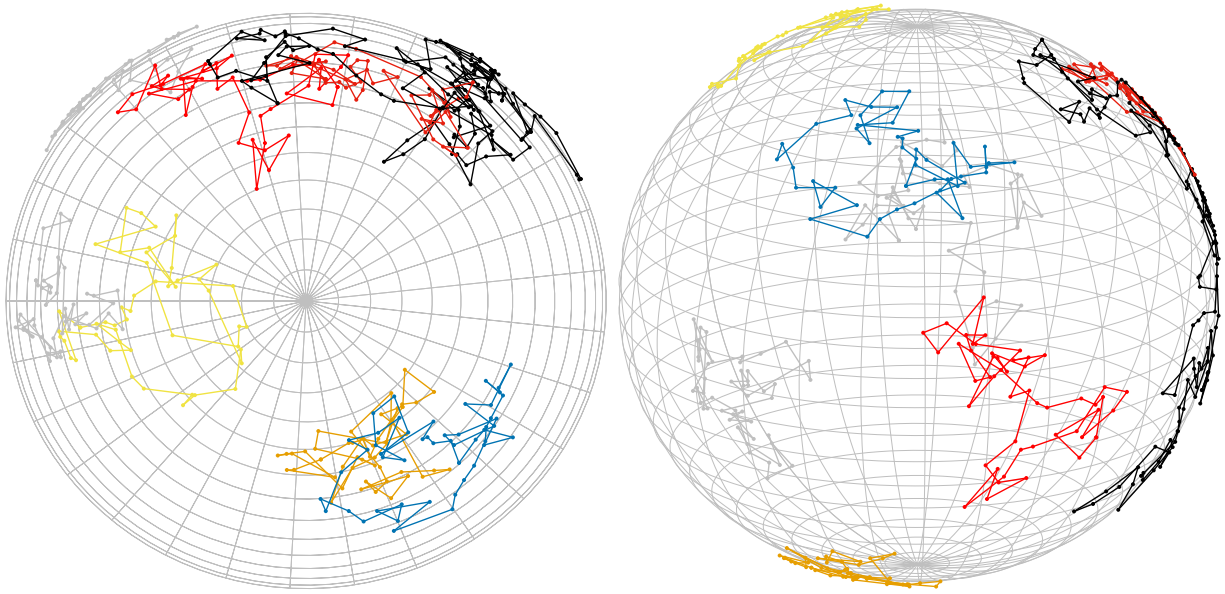

FIG. 1. Snapshot of the macroscopic path during the simulation for distinguishable non interacting particles with $M = 50, N = 10, a = 5, \beta = 1/10$. Case A in Table I. The different paths have different colors. In the left panel the top view and in the right panel the front view. In the simulation we measured $e_K = \langle \mathscr{K} \rangle = 1.04(4)$. Reducing β each path shrinks and tends to form a ring enclosing less amount of area.

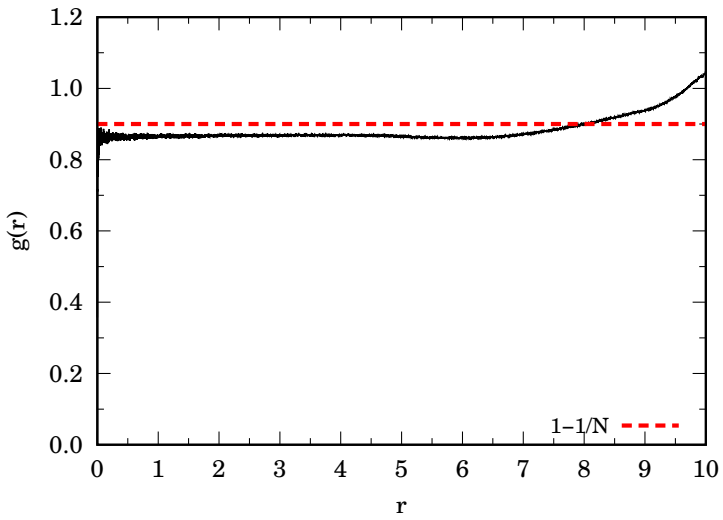

FIG. 2. The radial distribution function for the distinguishable non interacting gas with $N = 10$ on a sphere of radius $a = 5$ at an inverse temperature $\beta = 1/10$ with $M = 50$. Case A in Table I. The dashed line is for $g(r) = 1 - 1/N = 0.9$. The whirling upwards beyond $r > \sqrt{2a^2}$ is an artifact due to the choice of the Euclidean distance.

Bosons

Given the *superfluid* density σ_s and the *normal fluid* density $\sigma_n = 1 - \sigma_s$, the area estimator for the superfluid fraction is given by [11, 22]

$$f_s = \frac{\sigma_s}{\sigma} = 1 - \frac{\sigma_n}{\sigma} = \frac{2m\langle \mathscr{A}^2 \rangle}{\beta \lambda I_c}, \tag{4.1}$$

where, if ϵ is the Levi-Civita antisymmetric symbol,

$$\mathscr{A} = \frac{1}{2}\sum_{i,k} \epsilon_{\alpha\beta}(r_{i,k+1} - r_k)^\alpha (r_{i,k+2} - r_{k+1})^\beta \sqrt{g(\boldsymbol{r}_{i,k+1})}, \tag{4.2}$$

is the area occupied by all the single particle paths and $I_c = \frac{2}{3}Nm$ is the classical moment of inertia of a unit spherical shell of mass Nm.

In Fig. 3 we show a snapshot during the simulation for bosons non interacting particles with $M = 50, N = 10, a = 5, \beta = 1/10$. We see how the system forms 4 permutation cycles corresponding to different colors.

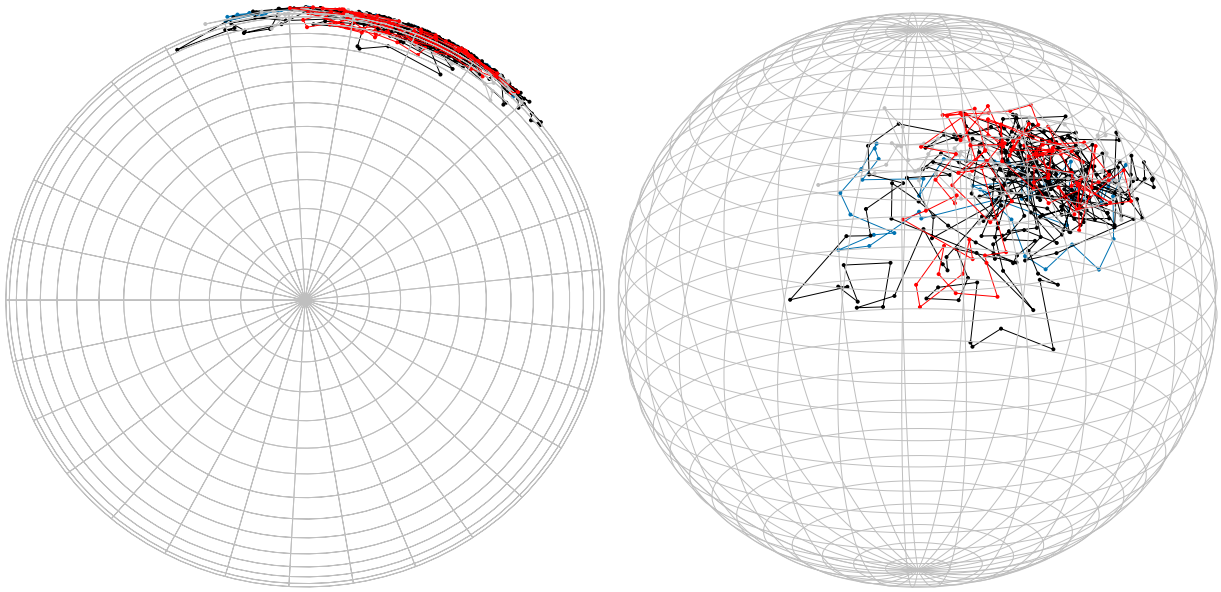

FIG. 3. Snapshot of the macroscopic path during the simulation for non interacting bosons with $M = 50, N = 10, a = 5, \beta = 1/10$. Case B in Table I. Paths corresponding to different permutations cycles have different colors. In the left panel the top view and in the right panel the front view. In the simulation we measured $e_K = \langle \mathscr{K} \rangle = -0.066(6)$. Reducing β each path shrinks and tends to form a ring enclosing less amount of area.

In Fig. 2 we show the radial distribution function, calculated by averaging the estimator of Eq. (3.5), for the bosons non interacting gas with $N = 10$ on a sphere of radius $a = 5$ at an inverse temperature $\beta = 1/10$ with $M = 50$. This is the same configuration used for Fig. 1. The bump at $r = 0$ is a consequence of condensation predicted by the Bose-Einstein statistics. Bosons like themselves.

FIG. 4. The radial distribution function for the bosons non interacting gas with $N = 10$ on a sphere of radius $a = 5$ at an inverse temperature $\beta = 1/10$ with $M = 50$. Case B in Table I. The dashed line is for $g(r) = 1 - 1/N = 0.9$. The bump at $r = 0$ is a manifestation of bosons to like themselves. The whirling upwards beyond $r > \sqrt{2a^2}$ is an artifact due to the choice of the Euclidean distance.

In Fig. 5 we show the superfluid fraction of Eq. (4.1) for the condensate of non interacting bosons with $N = 10, a = 5$, $M = 50$.

Fermions

Fermions properties cannot be calculated exactly with path integral Monte Carlo because of the fermions sign problem [14, 23]. We then have to resort to an approximated calculation. The one we chose was the restricted path integral approximation [1, 14, 23] with a "free fermions restriction". The trial density matrix used in the restriction is chosen as the one reducing to the ideal density matrix in the limit of $t \ll 1$ and is given by the following explicit

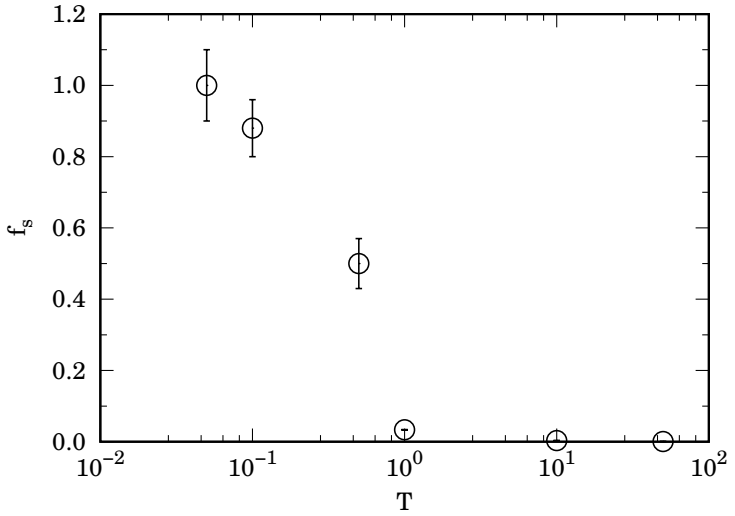

FIG. 5. The supefluid fraction (4.1) for the condensate of non interacting bosons with $N = 10, a = 5, M = 50$. In this case $\tau \leq 0.4$ and $T_D \approx 0.0318$.

analytic expression,

$$\rho_0(R', R; t) \propto \det \left|\left| e^{-\frac{ds^2(\boldsymbol{r}_i', \boldsymbol{r}_j)}{4\lambda t}} \right|\right|. \tag{4.3}$$

The *restricted path integral identity* that we will use states [14, 23]

$$\rho_F(R', R; \beta) \propto \int \sqrt{\tilde{g}''} dR''\, \rho_F(R'', R; 0) \int_{R'' \to R' \in \gamma_0(R)} \mathscr{D}R'''\, e^{-S[R''']}, \tag{4.4}$$

where S is the Feynman-Kac action

$$S[R] = \int_0^\beta dt \left[\frac{1}{4\lambda} \dot{R}_\mu \dot{R}^\mu + V(R) \right], \tag{4.5}$$

here the dot indicates a total derivative with respect to the imaginary thermal time, and the subscript in the path integral of Eq. (4.4) means that we restrict the path integration to paths starting at R'', ending at R' and avoiding the nodes of ρ_0, that is to the *reach* of R, $\gamma_0(R)$. The nodes are on the reach boundary $\partial\gamma_0$. The weight of the walk is $\rho_F(R'', R; 0) = \det||\delta(\boldsymbol{r}_i'' - \boldsymbol{r}_j)||$. Note that in imposing the restriction it is convenient to imagine an infinitely positive external potential which will prevent a transition move $R \to R'$ such that $\rho_0(R', R; \tau) < 0$ [13]. It is clear that the contribution of all the paths for a single element of the density matrix will be of the same sign, thus solving the sign problem; positive if $\rho_F(R'', R; 0) > 0$, negative otherwise. On the diagonal any density matrix is positive and on the path restriction $\rho_F(R', R; \beta) > 0$. Then only even permutations, those with $\mathrm{sgn}(\mathscr{P}) = +1$, are allowed, since $\rho_F(\mathscr{P}R, R; \beta) = \mathrm{sgn}(\mathscr{P})\rho_F(R, R; \beta)$. It is then possible to use a bosons calculation to get the fermions case. Clearly the restricted path integral identity with the free fermions restriction becomes exact if we simulate free fermions, but otherwise is just an approximation.

In Fig. 6 we show the radial distribution function, calculated by averaging the estimator of Eq. (3.5), for the fermions non interacting gas with $N = 10$ on a sphere of radius $a = 5$ at an inverse temperature $\beta = 1/10$ with $M = 50$. This is case C of Table I. The well at $r = 0$ is a consequence of Pauli exclusion principle predicted by the Fermi-Dirac statistics. Fermions dislike themselves.

---

[13] So that a move that changes the sign of ρ_0 are rejected in the Metropolis scheme.

FIG. 6. The radial distribution function for the fermions non interacting gas with $N = 10$ on a sphere of radius $a = 5$ at an inverse temperature $\beta = 1/10$ with $M = 50$. Case C in Table I. The dashed line is for $g(r) = 1 - 1/N = 0.9$. The hole at $r = 0$ is a manifestation of fermions to dislike themselves due to the Pauli exclusion principle. The whirling upwards beyond $r > \sqrt{2a^2}$ is an artifact due to the choice of the Euclidean distance.

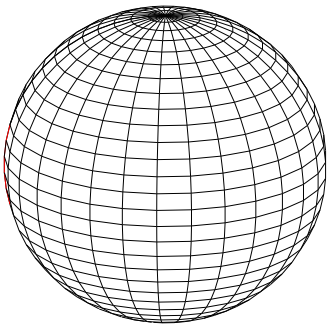

FIG. 7. ...

Anyons

Here we use the Metropolis algorithm with the transition displacement moves of Eqs. (A1) and (A2) and bridge moves of Eqs. (B1) and (B2) between unlike particles as described in Appendix C counting at each 2 bridges transition the number of single particles crossings in the newly generated R.

V. ELECTRON GAS

In this section we will study a system of electrons, i.e. spin $s = 1/2, g_s = 2$ fermions interacting through the Coulomb potential of Eq. (3.4). We will use the restricted path integral method described in subsection "Fermions" of Sec. IV B which is expected to become better at low density and high temperature, i.e. when correlation effects are weak.

Appendix A: The transition displacement move

In order to explore the θ and φ configuration space $\mathscr{C} =]-\pi/2, \pi/2] \times]-\pi, \pi]$ on the sphere it is convenient to propose the following transition move for each particle in a randomly chosen bead

$$\theta_{\rm new} = \theta_{\rm old} + \Delta_\theta(\eta - 1/2), \tag{A1}$$

$$\varphi_{\rm new} = \varphi_{\rm old} + \Delta_\varphi(\eta - 1/2), \tag{A2}$$

where $\eta \in [0, 1]$ is a uniform pseudo random number and Δ_θ and Δ_φ are two positive quantities measuring the θ-displacement and the φ-displacement respectively.

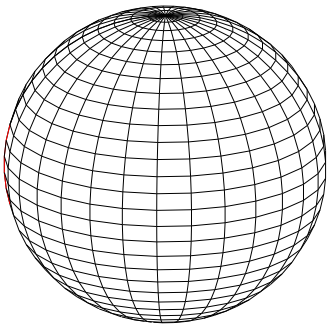

FIG. 8. Snapshot of the macroscopic path during the simulation. Paths belonging to different homotopy classes have different colors.

FIG. 9. The radial distribution function for the electron gas ..... with $N = 10$ on a sphere of radius $a = 5$ at an inverse temperature $\beta = 1/10$ with $M = 50$. Case A in Table I. The distance between a pole and a point on the equator is $\sqrt{50}$.

This transition move can bring $\boldsymbol{r}_{\rm new}$ out of $\mathscr{C}$ so it is also necessary to bring it back into $\mathscr{C}$ enforcing periodic boundary conditions $\varphi = \varphi + 2\pi$ and $\theta = \theta + \pi$ with the following subsequent chain of transformations

$$\begin{cases} \theta_{\rm new} \to \theta_{\rm new} - \pi \ \texttt{NINT}(\theta_{\rm new}/\pi), \\ \varphi_{\rm new} \to \varphi_{\rm new} - 2\pi \ \texttt{NINT}(\varphi_{\rm new}/2\pi), \end{cases} \tag{A3}$$

where NINT is the nearest integer function. One can easily convince himself that this chain does not alter the uniformity of the probability distribution of $\boldsymbol{r}_{\rm new}$ in $\mathscr{C}$.

Note that the metric enters the free particle variance since it is not possible by a change of coordinates to remove it both from the kinetic-action and from the integration measure $\sqrt{g(\boldsymbol{r})}\, d\boldsymbol{r}$, if not only locally. In order to take care of the metric factor in the integration measure it is convenient to introduce an effective/external single particle potential $\ln \sqrt{g(\boldsymbol{r})}$.

In the simulation we choose Δ_θ and Δ_φ so to have acceptance ratios as close as possible to 1/2 in the acceptance/rejection choices for the random walk transition displacement moves of the Metropolis algorithm. The transition probability distribution function for the displacement move of the Metropolis algorithm will be uniform so it will drop out of the acceptance probability distribution function.

Appendix B: The transition bridge move

In order to take into account the particles permutations it is necessary to construct two Brownian bridges between two different [14] randomly chosen particles in two randomly chosen beads to generate an exchange between the two particles. With one bridge we connect particle 1 on bead R_i to particle 2 on bead R_j and with the other we connect particle 2 on bead R_i to particle 1 on bead R_j with $i < j$. This will produce an *exchange* of particles 1 and 2.

[14] A bridge between the same particle can still be used to sample the density matrix of distinguishable particles as can be done the displacement move of Appendix A.

The Brownian bridge between particle l at $\boldsymbol{r}_{l,i}$ and particle m at $\boldsymbol{r}_{m,j}$ is built like so [11],

$$\boldsymbol{r}_{\mathrm{new},i} = \boldsymbol{r}_{l,i} \tag{B1}$$

$$\boldsymbol{r}_{\mathrm{new},k} = \boldsymbol{r}_{\mathrm{new},k-1} + \frac{(\boldsymbol{r}_{m,j} - \boldsymbol{r}_{\mathrm{new},k-1})}{j-k+1} + \boldsymbol{\xi}(\boldsymbol{r}_{\mathrm{new},k-1}) \quad k = i+1, \ldots, j-1 \tag{B2}$$

where $\xi^{\alpha}(\boldsymbol{r})$ is a random number with a Gaussian probability distribution with variance $\sigma^2_{\alpha\alpha}(\boldsymbol{r})(j-k)/(j-k+1)$ where $\sigma^2_{\alpha\alpha}(\boldsymbol{r}) = 2\lambda\tau/g_{\alpha\alpha}(\boldsymbol{r})$ is the diagonal free particle variance. In order to produce an exchange of two *unlike* particles l and m with $l \neq m$ one needs a 2 bridges transition as described above.

At each accepted transition, it is then necessary to bring the $\boldsymbol{r}_{\mathrm{new}}$ back into the region $\mathscr{C}$ through the transformations chain of Eq. (A3) in Appendix A.

Note that the metric enters the free particle variance since it is not possible by a change of coordinates to remove it both from the kinetic-action and from the integration measure $\sqrt{g(\boldsymbol{r})}\,d\boldsymbol{r}$, if not only locally. Even for the non interacting system, one would still need to adopt Metropolis algorithm in order to sample additionally the metric factor in the integration measure that can be seen as giving rise to an effective/external single particle potential $\ln\sqrt{g(\boldsymbol{r})}$. The transition probability distribution function of the Metropolis will be Gaussian.

Any permutation can be reached through a two particles exchange so the bridge transition move allows to sample the sum in Eq. (2.17).

Appendix C: Combination of bridges and diaplacements

In order to calculate each ρ_α in Eq. (2.19) one needs to combine bridges (described in Appendix B) and displacements (described in Appendix A). In fact one can first use bridge moves to reach the α homotopy class, with a fixed number n of braids, and then use only displacement moves to sample that particular ρ_α.

In order to sample the sum in Eq. (2.19) one needs to explore all possible swaps of two particles between any two timeslices i and j and at the same time count the number n of braids reached in the path $R(t)$ in order to be able to asses which path homotopy class he accessed after each move. This will allow him to determine to which ρ_α he is contributing at each accepted transition move.

If two different particles, say 1 and 2, have k crossings between timeslices i and $j > i$, an acceptance of the move described in Appendix B, where we build a bridge connecting $\boldsymbol{r}_{1,i}$ to $\boldsymbol{r}_{2,j}$ and one connecting $\boldsymbol{r}_{2,i}$ to $\boldsymbol{r}_{1,j}$, will necessarily result in just a single crossing if k is even, and consequently $n \to n-k+1$, or to no crossings at all, if k is odd, and consequently $n \to n-k$. In order to count the number of crossings between timeslices i and j it is necessary to count the number of times in which $\boldsymbol{r}_{1,k} = \boldsymbol{r}_{2,k}$ for $k \in [i,j]$. In order to take into account of this crossing condition in the discretized imaginary time one can for example determine when both $r^{\alpha}_{1,k} - r^{\alpha}_{2,k}$ for $\alpha = 1,2$ change sign varying k.

AUTHOR DECLARATIONS

Conflicts of interest

None declared.

Data availability

The data that support the findings of this study are available from the corresponding author upon reasonable request.

Funding

None declared.

[1] R. Fantoni, One-component fermion plasma on a sphere at finite temperature, Int. J. Mod. Phys. C **29**, 1850064 (2018).

[2] R. Fantoni, One-component fermion plasma on a sphere at finite temperature. The anisotropy in the paths conformations, J. Stat. Mech. , 083103 (2023).

[3] G. O. V. Melik-Alaverdian, N. E. Bonesteel, Fixed-phase diffusion Monte Carlo study of the quantum-Hall effect on the Haldane sphere, Physica E **1**, 138 (1997).

[4] G. O. V. Melik-Alaverdian, N. E. Bonesteel, Quantum Hall Fluids on the Haldane Sphere: A Diffusion Monte Carlo Study, Phys. Rev. Lett. **79**, 5286 (1997).

[5] N. E. B. V. Melik-Alaverdian, G. Ortiz, Quantum Projector Method on Curved Manifolds, Phys. Rev. Lett. 10.48550/arXiv.cond-mat/0001121 (1997), arXiv:cond-mat/0001121.

[6] J. R. Klauder and R. Fantoni, The Magnificent Realm of Affine Quantization: valid results for particles, fields, and gravity, Axioms **12**, 911 (2023).

[7] B. S. DeWitt, Dynamical Theory in Curved Spaces. I. A Review of the Classical and Quantum Action Principles, Rev. Mod. Phys. **29**, 377 (1957).

[8] J. H. V. Vleck, The Correspondence Principle in the Statistical Interpretation of Quantum Mechanics, Proc Natl Acad Sci U S A **14**, 178 (1928).

[9] L. S. Schulman, *Techniques and Applications of Path Integration* (John Wiley & Sons, Technion, Haifa, Israel, 1981) chapter 24.

[10] H. F. Trotter, On the Product of Semi-Groups of Operators, Proc. Am. Math. Soc. **10**, 545 (1959).

[11] D. M. Ceperley, Path integrals in the theory of condensed Helium, Rev. Mod. Phys. **67**, 279 (1995).

[12] F. Bastianelli and O. Corradini, On the simplified path integral on spheres, Eur. Phys. J. C **77**, 731 (2017).

[13] C. W. Misner, K. S. Thorne, and J. A. Wheeler, *Gravitation* (W. H. Freeman, San Francisco, 1973).

[14] D. M. Ceperley, Path integral Monte Carlo methods for fermions, in *Monte Carlo and Molecular Dynamics of Condensed Matter Systems*, edited by K. Binder and G. Ciccotti (Editrice Compositori, Bologna, Italy, 1996).

[15] A. Lerda, *Anyons. Quantum Mechanics of Particles with Fractional Statistics* (Springer-Verlag, Berlin, 1992).

[16] N. Metropolis, A. W. Rosenbluth, M. N. Rosenbluth, A. M. Teller, and E. Teller, Equation of state calculations by fast computing machines, J. Chem. Phys. **1087**, 21 (1953).

[17] M. H. Kalos and P. A. Whitlock, *Monte Carlo Methods* (John Wiley & Sons Inc., New York, 1986).

[18] E. A. Abbott, *Flatland: A Romance of Many Dimensions* (Seeley & Co., London, 1884).

[19] R. Fantoni, B. Jancovici, and G. Téllez, Pressures for a One-Component Plasma on a Pseudosphere, J. Stat. Phys. **112**, 27 (2003).

[20] R. Fantoni and G. Téllez, Two dimensional one-component plasma on a Flamm's paraboloid, J. Stat. Phys. **133**, 449 (2008).

[21] R. Fantoni, Two component plasma in a Flamm's paraboloid, J. Stat. Mech. , P04015 (2012).

[22] E. L. Pollock and D. M. Ceperley, Path-integral computation of superfluid densities, Phys. Rev. B **36**, 8343 (1987).

[23] D. M. Ceperley, Fermion Nodes, J. Stat. Phys. **63**, 1237 (1991).